

PREPRINT 2007:16

Envelope Crossing Distributions for Gaussian Fields

KRZYSZTOF PODGÓRSKI
IGOR RYCHLIK

Department of Mathematical Sciences
Division of Mathematical Statistics
CHALMERS UNIVERSITY OF TECHNOLOGY
GÖTEBORG UNIVERSITY
Göteborg Sweden 2007

Preprint 2007:16

Envelope Crossing Distributions for Gaussian Fields

Krzysztof Podgórski and Igor Rychlik

CHALMERS | GÖTEBORG UNIVERSITY



Department of Mathematical Sciences
Division of Mathematical Statistics
Chalmers University of Technology and Göteborg University
SE-412 96 Göteborg, Sweden
Göteborg, June 2007

Preprint 2007:16
ISSN 1652-9715

Matematiska vetenskaper
Göteborg 2007

ENVELOPE CROSSING DISTRIBUTIONS FOR GAUSSIAN FIELDS

KRZYSZTOF PODGÓRSKI AND IGOR RYCHLIK

ABSTRACT. The envelope process is an analytical tool often used to study extremes and wave groups. In an approach to approximate the first passage probability for the underlying response the average number of envelope crossings is used to obtain an upper bound. Vanmarcke (1975) improved this approximation by accounting for the proportion of empty excursions of the envelope. Ditlevsen and Lindgren (1988) proposed an accurate approximation of this proportion by using the Slepian model method. This approximation was further studied in Ditlevson (1994). In the first part of the paper, we review the approach as well as give a brief account of the results.

In the second main part of the paper, the method of sampling distribution is applied to the envelope field that is a generalization of the envelope process. The need of considering a field rather than a process is particularly important in these applications for which both spatial and temporal variability has to be taken into account. Here we notice that the envelope field is not uniquely defined and that its statistical properties depend on a chosen version. We utilize convenient envelope sampling distributions to decide for a version that has desired smoothing properties. The spatial-temporal Gaussian sea-surface model is used to illustrate this approach.

One intrinsically multivariate problem is studying velocities of moving spatial records. It is particularly important in marine applications as the velocity of the envelope is related to the rate at which energy is transported by propagating waves. Under the Gaussian model we derive sampling properties of the envelope velocity measured at the level contours. By associating the properties of envelope with the properties of group waves we present differences between statistical distributions of individual waves and waves groups.

1. INTRODUCTION

In his pioneering work Longuet-Higgins (1957) has introduced the decomposition of traveling random waves into the envelope (low frequency varying amplitude) and the carrier (high frequency oscillations). The envelope is always above the underlying signal and typically smoothes it out, therefore its average number of crossings is often used to conveniently

approximate distributions of the global maximum. For marine applications the envelope is used in connection with statistical analysis of wave crests and wave groups while in fatigue analysis it is used to obtain fatigue damage approximations through the rainflow method.

The envelope is defined as the norm of the complex process with the underlying signal as its real component and the Hilbert transform as its imaginary part. The envelope is typically smoother than the underlying process while at high levels it generally follows its height. This is due to the fact that the Hilbert transform (if properly defined) is strongly correlated with the derivative of the signal and thus it is approximately equal to zero at the extrema. Consequently the high levels are exceeded by the envelope if they are exceeded by the signal and often vice versa. If this is not the case, then the envelope upcrosses a level while the underlying signal stays below throughout the entire envelope excursion that is then described as an *empty* one. The average number of upcrossing by the process is used as a standard upper bound for the distribution of the global maximum. If the envelope upcrossings are adjusted for the empty excursions their average number gives a more precise upper bound. This is due to smoothness of the envelope which results in an essentially smaller number of its non-empty, i.e. *qualified* crossings than the number of the crossings for the underlying signal. The idea was first explored in Vanmarcke (1975) and later in Ditlevsen and Lindgren (1988), Ditlevsen (1994), where the Slepian model of the process at the envelope upcrossing was used to approximate more accurately the proportion of empty excursions. In Section 3, we review this problem in further detail while presenting Ove Ditlevsen's contribution to this application of the envelope.

In analysis of safety of structure subjected to environmental loads one is estimating the probability that strength of components is larger than the maximal experienced load and that the material deterioration due to time variable loads is not decreasing its strength. Here the fatigue damage – cracking – is one of the most important material degradation processes. In the past envelope was used to approximate the risk for failure in both cases. For a stationary Gaussian process the distribution of the envelope is Rayleigh. The Rayleigh variable is commonly used in prediction of fatigue failure caused by wave induced loads (Gaussian processes) acting on the offshore structure. In particular, one is approximating the rate of the fatigue damage growth at a hot spot to be proportional to a moment of the envelope, where the proportionality constant depends on the structure geometry and material, while

the order of the moment is material dependent only. This approach was introduced in the pioneering work of Bendat (1966) who argued that envelope probability density is equivalent to peak probability density functions for narrow band Gaussian process. In Rychlik (1993) it was proven that Bendat's "narrow band" approximation is actually an upper bound for the damage rate computed by means of the rainflow method for any stationary Gaussian load. Bendat's approach has also been extended to any smooth stationary load for which the upcrossing intensity can be computed. In another fatigue application, Jiao and Moan (1990) consider wave loads for a typical situations of mixture of swell and wind driven sea. This leads to Gaussian loads with power spectra having well separated tops, i.e. the signal is made of a slowly varying load with added high frequency noise. The damage rate of such process is approximated by a sum of damages caused separately by the noise (narrow-band approximation was employed) and by the slowly varying part for which peaks were raised by the height of the envelope of the noise.

Another type of risks in offshore operations is the possibility of undesire responses of the vessels which can result in capsizing. This events have higher chances to occure if the speed of the vessel is comparable to the wave velocity and the time spend in a large wave group is long. Some aspects of this problem can be studied by analyzing the wave group velocity. The wave groups are defined, not quite precisely, as collections of waves with large ones in the center accompanied with small vanishing waves at the ends. The wave groups are observed in empirical data where often a high wave is preceded or succeeded by another wave which is higher than average. Properties of such groups are important for ocean engineers. For example, a group of waves can be responsible for a capsize of the ship if she will not regain stability between oncoming high waves in the group. It is often reported that groups of waves do more damage than waves of the same size but separated by smaller waves [see, for example, Burcharth (1980)]. This is partially explained by the fact that energy propagate with the rate corresponding to the speed of waves groups. For deep water waves this rate is slower than the speed of individual waves and it can be demonstrated by physical arguments that for waves having narrow band spectra it is the envelope that is responsible for the transport of energy.

Despite that in the original work of Longuet-Higgins the envelope was proposed for moving random surface, most of the future work was done for the envelope of univariate random

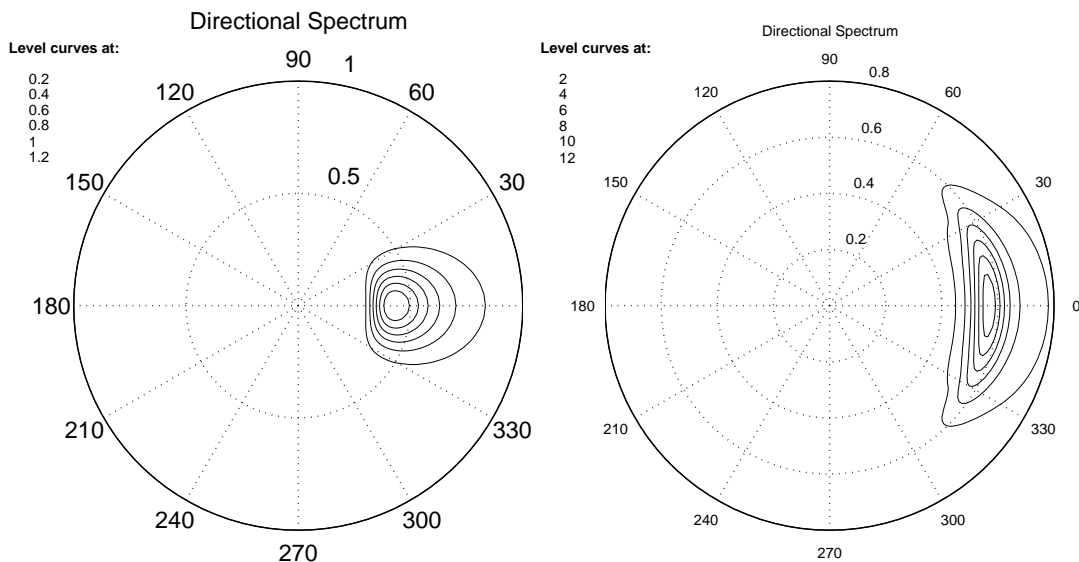


FIGURE 1. Examples of directional spectra: swell spectrum (left); JONSWAP spectrum used in examples (right).

processes with the notable exception of Adler (1978,1981), where the definition and some properties of the bivariate envelope field were discussed. We extend this original work and focus on applications to studies of Gaussian sea surfaces.

In truly two dimensional set-up where even individual waves are hard to describe in a formal manner, the notion of wave groups escapes a precise definition. On the other hand the envelope field is defined in an arbitrary dimension and its properties naturally extend from the one-dimensional case. Take for example the sea surface given by the swell spectrum shown in Figure 1, [details on the model of this spectrum can be found in Torsethaugen (1996)]. The difference between dynamics of surface and envelopes can be illustrated by recording contour movements in two time instants within $5[s]$. For each of the field, let us consider the contours crossing the significant crest height level (the significant wave height, in this case, is $2.2[m]$, thus the crossing level or the significant crest height is $1.1[m]$ above the mean sea level). For the sea surface, in order to obtain a more transparent picture of the contours we have also added crossing contours at the level equal to 90% of the significant wave crest. Several important features can be noticed from the graphs presented in Figures 2 where the waves are moving from right to left. First, the envelope field is indeed grouping the waves

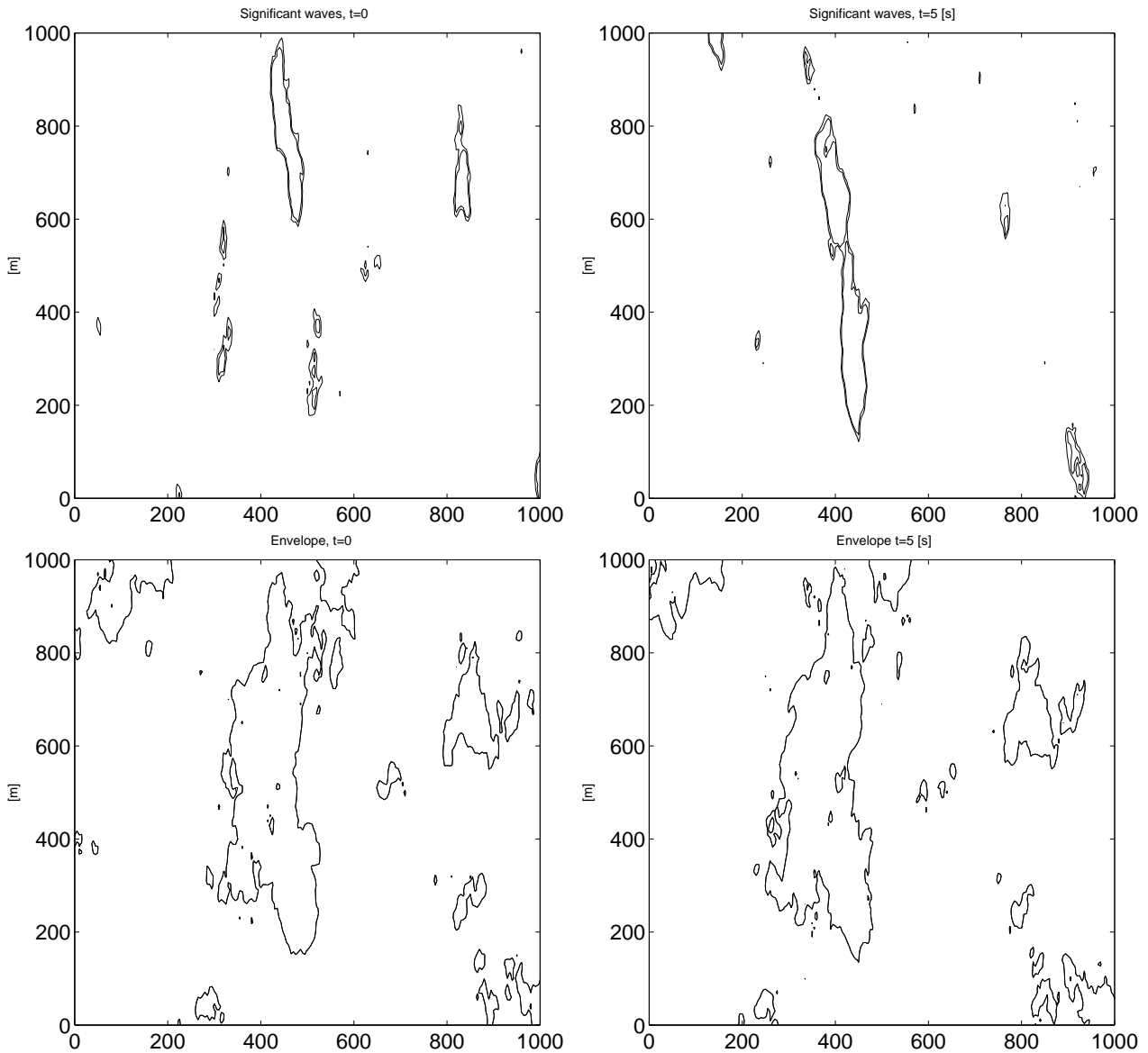


FIGURE 2. Motion of level crossing contours for sea surface (top) and envelope (bottom) – the principal direction of wave movement is from the right to the left.

as its contours cover areas in which we observe clearly separated contours of the sea surface. Next, the displacements for the envelope are evidently smaller than for the sea surface – the envelope appears to move slower than the sea surface. The level crossing contours for the envelope are more stable, appearing mostly to drift with no rapid change in shape or size. Note also that waves entering the envelope contours are growing while these which are leaving are diminishing – expected behavior when the waves group are moving slower than the individual waves.

In this paper, we analyze the envelope in a systematic way using statistical properties of this multivariate field. In Section 2, we outline the foundations of statistical distributions sampled at the level crossings of random fields that are based on the generalized Rice's formula. After that the problem of empty envelope excursions is formulated and Ditlevson's contributions is recapitulated. Then we devote some space to discuss the definition of the multivariate envelope which is not a unique concept. In fact there is certain freedom of a choice following from the definition of the envelope. Thus we start with a discussion of choices of the envelope for evolving sea surface. Later we derive some statistical distribution of properly defined velocities for the envelope. Finally, these distributions are compared with the analogous distributions obtained for the underlying sea surface in both analytical and numerical manner. Numerical computations are performed for a Gaussian sea having a JONSWAP directional spectrum. Our numerical studies are supported by the MATLAB toolbox WAFO – Wave Analysis in Fatigue and Oceanography – containing a comprehensive package of numerical subroutines and programs for statistical analysis of random waves. This toolbox is available free of charge at <http://www.maths.lth.se/matstat/wafo>.

2. STOCHASTIC FIELDS SAMPLED AT LEVEL CROSSINGS

Stochastic processes serve as probability models of phenomena observed in some continuum, for example in time or in space or sometimes in both. It is often assumed that observed realizations produced by a model or, as they are often called, *sample paths* contain all information about the model (ergodic property). Vice versa, the theoretical model can provide with formulas for the statistical distributions extracted from sample paths. However, the relation between the sample path distributions and the theoretical distributions describing the model is not always straightforward. For example, complications can arise from the effect of *sampling bias*. The name refers to a change of sample distribution for the same quantity due to a different method of collecting its values. Identifying the sampling distributions appropriate for specific applications is an important issue that is discussed here in more detail.

Let $X(\boldsymbol{\tau})$ be a stationary and ergodic random field. The probability that this field has a (measurable) property A is given by $\mathbf{P}(X \in A)$. These probabilities are referred to as the theoretical distribution of X . By the law of large numbers and ergodicity it also represents

statistical distributions of $X(\boldsymbol{\tau} + \cdot)$ sampled at completely randomly chosen $\boldsymbol{\tau}$ over large region of $\boldsymbol{\tau}$'s. For this reason it is often called the unbiased sampling distribution. Suppose now that one is interested in the property A only at the points $\boldsymbol{\tau}$ for which $|X(\boldsymbol{\tau})| \leq \epsilon$, for small $\epsilon > 0$, i.e. when $X \approx 0$. More precisely, if we consider the set $\{\boldsymbol{\tau} : |X(\boldsymbol{\tau})| \leq \epsilon\}$, and take a sample of its points using uniform distribution over this set, then the obtained distribution is well approximated by the conditional distribution $\mathbf{P}(X \in A | X(\mathbf{0}) = 0)$. It is a somewhat surprising and often confusing fact that if one samples observations uniformly from the contour set $\mathcal{C}_u = \{\boldsymbol{\tau}; X(\boldsymbol{\tau}) = u\}$, $u = 0$, then this distribution is not asymptotically equal to $\mathbf{P}(X \in A | X(\mathbf{0}) = 0)$. The restriction to contour sets that have a smaller dimension than the domain of the process introduces the *sampling bias*. The proper formulas for the biased sampling distributions are given in (2) and (3). A short account of the theory that leads to them follows.

In order to discuss biased sampling distributions, first we should answer the question of how large are the u -level crossing contours \mathcal{C}_u in the terms of the measure that parallels their dimension. In mathematics this measure is referred to as the Hausdorff measure and the corresponding dimension is called the Hausdorff dimension. For example, the Hausdorff dimension of a discrete set of points is equal to zero and its Hausdorff measure counts the number of points in the set, the Hausdorff dimension of a contour line on the plane equals one with the corresponding Hausdorff measure equal to the length of the line. Alternatively, we refer to the Hausdorff measure more descriptively as the relative volume of a set A and denote it by $\mathcal{V}(A)$ without indicating explicitly the dependence on the Hausdorff dimension. The mean sizes of level crossing contour in the terms of their relative volumes is given by the celebrated Rice formula [Rice (1944),(1945)].

Originally it was formulated as a one dimensional version of the problem, i.e. when X depends only on one variable, say, t in which the case the contours are made of discrete points. It states that $\mathcal{V}(\mathcal{C}_u \cap [0, T])$ (which in this case is simply the number of times X takes the value u in $[0, T]$), when divided by increasing without bound T , with probability one converges to

$$(1) \quad \int |y| f_{\dot{X}(0), X(0)}(y, u) dy = \mathbf{E} \left(|\dot{X}(0)| \mid X(0) = u \right) \cdot f_{X(0)}(u),$$

where $f_{\dot{X}(0), X(0)}$, $f_{X(0)}$ are the density functions of $(\dot{X}(0), X(0))$ and $X(0)$, respectively. The above formulation is valid under the assumptions of stationarity and ergodicity of X and is a combination of the ergodic theorem and the original Rice formula, which stated that the average number of crossing $N(1)$, i.e. $\mathbf{E}(N(1))$ equals the left hand side of (1).

There is an extension of the above result for the number of times t such that $X(t) = u$ in $[0, T]$ and at the same time the process $X(t + \cdot)$ has a property A (here the property A may even apply to the entire trajectory of the process $s \mapsto X(t + s)$). Namely, we have with probability one

$$(2) \quad \lim_{T \rightarrow \infty} \frac{\mathcal{V}(\mathcal{C}_u \cap \{t \in \mathbb{R} : X(t + \cdot) \in A\})}{\mathcal{V}(\mathcal{C}_u)} = \frac{\mathbf{E}(\{X \in A\} \dot{X}(0) | X(0) = u)}{\mathbf{E}(|\dot{X}(0)| | X(0) = u)},$$

where the set $\{X \in A\}$ is identified with its indicator function, i.e. a function that takes one if argument is in the set and zero otherwise. Consequently, the right hand side represents the biased sampling distribution when sampling is made uniformly from the u -level contour \mathcal{C}_u . We use the following notation for this distribution

$$\mathbf{P}(X \in A | \mathcal{C}_u) = \mathbf{P}(X(t + \cdot) \in A | t \in \mathcal{C}_u)$$

and refer to it as the distribution of X on the contour \mathcal{C}_u .

The extension to the multivariate case is fairly straightforward. Consider a pair of jointly stationary stochastic processes $\mathbf{V}(\mathbf{p})$, $\mathbf{X}(\mathbf{p})$, $\mathbf{p} \in \mathbb{R}^k$, taking values in \mathbb{R}^m and \mathbb{R}^n , respectively. Assume that $n \leq k$ and from now on treat them as fixed. Further let \mathcal{V} stand for the relative volume in \mathbb{R}^k of the dimension $k - n$ (as before if $k = 3$, then \mathcal{V} represents the length of a set if $n = 2$, the area if $n = 1$, and \mathcal{V} simply counts points in a set in the special case $n = 3$). The distribution of $\mathbf{V}(\mathbf{p})$ on the contour $\mathcal{C}_\mathbf{u} = \{\mathbf{p} \in [0, 1]^k : \mathbf{X}(\mathbf{p}) = \mathbf{u}\}$ is given by

$$(3) \quad \mathbf{P}(\mathbf{V}(\mathbf{p}) \in A | \mathbf{p} \in \mathcal{C}_\mathbf{u}) \stackrel{def}{=} \frac{\mathbf{E}[\mathcal{V} \{ \mathbf{p} \in \mathcal{C}_\mathbf{u} : \mathbf{V}(\mathbf{p}) \in A \}]}{\mathbf{E}[\mathcal{V}(\mathcal{C}_\mathbf{u})]}.$$

A generalized Rice formula is utilized to compute this distribution. Let $\mathbf{X}(\mathbf{p})$ have continuous finite dimensional distributions and denote by $f_{\mathbf{X}(\mathbf{0})}(\mathbf{u})$ the density of $\mathbf{X}(\mathbf{0})$. Let $\dot{\mathbf{X}}(\mathbf{p})$ be the matrix of partial derivatives of $\mathbf{X}(\mathbf{p})$ (which are assumed to exist). The generalized determinant of this matrix is denoted by $\det(\dot{\mathbf{X}}(\mathbf{p}))$. Use of the above notation allows us to

write a generic form of the Rice formula as

$$(4) \quad \mathbb{E}[\mathcal{V}\{\mathbf{p} \in \mathcal{C}_{\mathbf{u}} : \mathbf{V}(\mathbf{p}) \in A\}] = \mathbb{E}\left(\{\mathbf{V}(\mathbf{0}) \in A\} \cdot \det \dot{\mathbf{X}}(\mathbf{0}) \mid \mathbf{X}(\mathbf{0}) = \mathbf{u}\right) f_{\mathbf{X}(\mathbf{0})}(\mathbf{u}).$$

Notice that if the joint density of \mathbf{V} , \mathbf{X} , $\dot{\mathbf{X}}$ is available, which is always the case in this paper, the right hand side can be written simply in the form of an integral and the biased sampling distribution can be written as

$$(5) \quad \mathbb{P}(\mathbf{V}(\mathbf{p}) \in A \mid \mathbf{p} \in \mathcal{C}_{\mathbf{u}}) = \frac{\int_A \int f_{\mathbf{V}, \dot{\mathbf{X}}, \mathbf{X}}(\mathbf{v}, \dot{\mathbf{x}}, \mathbf{u}) \cdot \det \dot{\mathbf{x}} \, d\dot{\mathbf{x}} d\mathbf{v}}{\int f_{\dot{\mathbf{X}}, \mathbf{X}}(\dot{\mathbf{x}}, \mathbf{u}) \cdot \det \dot{\mathbf{x}} \, d\dot{\mathbf{x}}}.$$

See Appendix C for details and further extensions.

In the context of the present paper, the process $\mathbf{V}(\mathbf{p})$ may represent a velocity measured at a spatial point \mathbf{p} . Velocity can be vector valued or scalar (speed) and thus either $m = 2$ or $m = 1$. The process $\mathbf{X}(\mathbf{p})$ may represent either the envelope field $E(\mathbf{p})$ or the underlying sea surface $W(\mathbf{p})$. The distributions of velocities can be considered for sampling on a level crossing contour of $E(\mathbf{p})$, in which case $n = 1$ and $k = 2$. The determinant $\det \dot{\mathbf{E}}$ is then equal to $\|\dot{\mathbf{E}}\| = \sqrt{E_x^2 + E_y^2}$ and \mathcal{V} measures the length of the contour on the plane.

A type of biased sampling distributions can be dictated by the nature of the problem in hand and can be essentially different from the ones discussed in this work. Our presentation merely illustrate techniques of deriving theoretical forms of distributions sampled at various cases of contours. The derivation should help to approach problems of finding sampling distributions on contours in many other multivariate situations of practical interest.

3. GLOBAL MAXIMUM AND EMPTY ENVELOPE EXCURSIONS

In engineering applications such as safety analysis of offshore structures, the distribution of maximum of a signal $X(t)$ is of interest. The Rice method uses the following upper bound for the distribution of the maximum

$$(6) \quad \mathbb{P}(M_T > u) \leq \mathbb{P}(X(0) > u) + \mathbb{P}(N_T^+(u) > 0) \leq \mathbb{P}(X(0) > u) + \mu^+(u) \cdot T,$$

where $M_T = \max_{0 \leq t \leq T} X(t)$, $N_T^+(u) = \#\{t \in [0, T] : X(t) = u, \dot{X}(t) > 0\}$ and the upcrossing intensity $\mu^+(u) = \mathbb{E}(N_T^+(u)) / T$. (Here and in what follows $\#(A)$ stands for the number of elements of a set A .) For a stationary process X the celebrated Rice formula states that

$$\mu^+(u) = \mathbb{E}\left(\dot{X}^+(0) \mid X(0) = u\right) f_{X(0)}(u),$$

where $x^+ = \max(0, x)$ and $f_{X(0)}$ is the density of $X(0)$. Thus in the Gaussian zero mean case

$$\mu^+(u) = \frac{1}{2\pi} \sqrt{\frac{\lambda_2}{\lambda_0}} e^{-\frac{u^2}{2\lambda_0}},$$

where λ_i 's are the spectral moments of the process, i.e. if σ is the spectral measure so the covariance function $R(t) = \text{COV}(X(t), X(0)) = \int_{-\infty}^{\infty} e^{it\lambda} d\sigma(\lambda)$, then

$$\lambda_i = 2 \int_0^{\infty} \lambda^i d\sigma(\lambda).$$

The quantity $T_2 = 2\pi \sqrt{\frac{\lambda_0}{\lambda_2}}$ represents the expected (mean) period of X and thus

$$\mu^+(u) = \frac{e^{-\frac{u^2}{2\lambda_0}}}{T_2}$$

with the zero ($u = 0$) upcrossing intensity being the reciprocal of the period T_2 . The term $\text{P}(X(0) > u)$ in (6) can be neglected if the level u is large (the most interesting case for applications) and T is larger than the period T_2 . In this situation the process typically crosses the u level more than once, in particular when a group of waves has approached. Consequently, the second term in (6) becomes a very crude upper bound.

An apparent wave group is difficult to define rigorously although for a narrow band process (swell) groups of waves are clearly seen in the records. They can be fairly well identified through subsequent crossings of high level by the envelope that is defined as

$$E(t) = \sqrt{X^2(t) + X_H^2(t)},$$

where $X_H(t)$ is Hilbert transform of $X(t)$ (see the Appendices for the details). The envelope $E(t)$ is always above the process $X(t)$ thus we have an obvious relation

$$\text{P}(N_T^+(u) > 0) \leq \text{P}(E(0) > u) + \text{P}(\mathcal{N}_T^+(u) > 0),$$

where $\mathcal{N}_T^+(u)$ stands for upcrossings of the envelope. The above can be improved using the number $\mathcal{N}_{0,T}^+(u)$ of empty envelope excursions

$$\text{P}(N_T^+(u) > 0) = \text{P}(E(0) > u) + \text{P}(\mathcal{N}_T^+(u) - \mathcal{N}_{0,T}^+(u) > 0) \leq \text{P}(E(0) > u) + \text{E}(\mathcal{N}_T^+(u)) - \text{E}(\mathcal{N}_{0,T}^+(u)).$$

In view of the preceding comments, the following upper bound may lead to an improvement over (6):

$$(7) \quad \text{P}(M_T > u) \leq \text{P}(X(0) > u) + (\nu^+(u) - \nu_0^+(u)) \cdot T,$$

where ν^+ and ν_0^+ are the envelope intensities of upcrossings and empty upcrossings, respectively.

The intensities of upcrossings of the envelope and its empty excursions can be expressed using polar coordinates $(E(t), \theta(t))$ of $(X(t), X_H(t))$:

$$X(t) = E(t) \cos \theta(t),$$

$$X_H(t) = E(t) \sin \theta(t).$$

Defining $Z(t) = E^2(t)$ the intensity $\nu^+(u)$ of upcrossing of the envelope is given by

$$\nu^+(u) = \mathbf{E} \left(\dot{Z}^+(0) \mid Z(0) = u^2 \right) f_{Z(0)}(u^2).$$

The density of $Z(0)$ is exponential with the intensity $1/(2\lambda_0)$ and

$$f_{Z(0)}(u^2) = \frac{1}{2\lambda_0} e^{-\frac{u^2}{2\lambda_0}}.$$

The conditional distribution of $\dot{Z}(0) = 2\dot{X}(0)X(0) + 2\dot{X}_H(0)X_H(0)$ given $E(0) = u$ and $\theta(0) = \theta$ is normal with mean zero and the variance

$$\text{Var} \left(\dot{Z}(0) \mid E(0) = u, \theta(0) = \theta \right) = 4u^2 \lambda_2 (1 - \rho^2),$$

where $\rho^2 = \lambda_1^2 / (\lambda_0 \lambda_2)$ is the squared correlation between the derivative $\dot{X}(t)$ of the process and its Hilbert transform $X_H(t)$. The parameter $\gamma = \sqrt{1 - \rho^2}$ is known in the literature as the *spectral width* of the process. Here we note that the high correlation of the derivative and Hilbert transform may lead to the envelope nearly touching process at local extrema of the process – a “small” value of the Hilbert transform typically will correlate with a zero of the derivative. Consequently, one should expect the narrow bandness to be related to the small rates of empty envelopes excursions at high levels. We also observe independence of $\theta(0)$ and thus

$$\nu^+(u) = \sqrt{\frac{2\pi(1 - \rho^2)}{\lambda_0}} \cdot u \cdot \frac{e^{-\frac{u^2}{2\lambda_0}}}{T_2}.$$

Evaluating $\nu_0^+(u)$ that is used in (7) is a more challenging task. One way to approach to the problem is to applied a generalized Rice formula to obtain sampling distribution of an envelope excursion to be empty and thus computing $\nu_0^+(u)/\nu^+(u)$. Despite this relatively straightforward formulation of the problem, the actual computation requires further generalizations of Rice’s formula as compared to the one given in (5). Such an approach is further

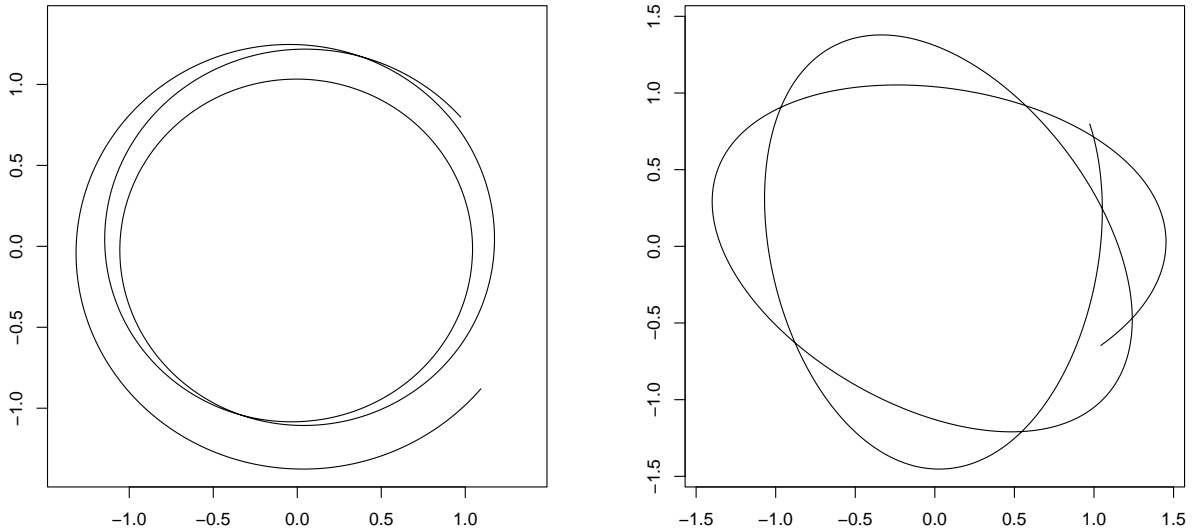


FIGURE 3. Complex envelope for the “narrow band” (*left*) and the “broad band” (*right*) cases. We observe lower rate of empty envelope excursions for the “narrow band” case ($\rho^2 = 0.99$) than for the “broad band” case ($\rho^2 = 0.60$).

discussed in Appendix C. Another approach that allows for approximation and simplification this computationally difficult problem has been successfully implemented in Ditlevson and Lindgren (1988). The method is based on the Slepian model at envelope upcrossing that is described below.

The empty envelope excursions occur at t instants such that $E(t) = u$ and $\dot{E}(t) > 0$ and $E(s) \cos \theta(s) < u$ for $s \in (t, \min\{s > t; E(s) \leq u\})$ before $E(s)$ goes again under u for $s > t$, i.e. when the complex envelope $\mathcal{E}(t) = X(t) + iX_H(t)$ after leaving the circle of radius u stays in the half-plane $\{z; \Re(z) < u\}$ until its subsequent return inside the circle. In Figure 3 we see examples of the complex envelope with low and high rates of empty excursions.

Let us consider the conditioning of the process around exit of the circle with radius u of the complex envelope $\mathcal{E}(t)$ so the only stochastic contribution to the resulting excursion comes from the angle ϕ at which the crossing occurs. There exists the unique interval $(\phi, \phi + \delta)$ of the minimal length such that the entire excursion of the envelope is contained between the tangent lines to the circle set at the angles ϕ and $\phi + \delta$. Because of the rotational invariance of the complex envelope distribution under the considered conditioning the distribution of the angle ϕ is uniform on interval $(0, 2\pi)$ while δ is fixed, non-random. Consequently, a qualified excursion occurs if this interval contains the zero angle, i.e. upon the considered

conditioning it is equal to $\delta/(2\pi)$. In general the unconditional distribution of δ is very complicated. In Ditlevson and Lindgren (1988) it is argued that for narrow band processes, i.e. when the correlation ρ is high, the angular interval $(\phi, \phi + \delta)$ is approximately equal to the angular interval of the complex envelope excursion from the circle. Then the problem can be simplified even further by assuming that for narrow band processes the interval of the excursion for the process can be well approximated by its mean value evaluated at the exit point of the circle. Through this simplification of the problem δ is approximated by the length of excursion of the averaged process that stochastically depends only on the velocity of the complex envelope process at the exit time.

More precisely, the complex process $\mathcal{E}(t)$ conditionally on $Z(0) = u^2, \theta(0) = \theta, \dot{Z}(0) = \dot{z}$ is equivalent to conditioning on $X(0) = u \cos \theta, Y(0) = u \sin \theta, 2u(\dot{X}(0) \cos \theta + \dot{Y}(0) \sin \theta) = \dot{z}$. Thus it corresponds to the distribution of a bivariate Gaussian process $\mathbf{E}(t)$ with the mean $\mathbf{m}(t; u, \theta, \dot{z})$ and covariance structure $\Sigma(t, s; \theta)$ depending neither on u nor on \dot{z} . Let us define a residual process

$$\mathbf{E}_\theta(t) = \mathbf{E}(t) - \mathbf{m}(t; u, \theta, \dot{z}).$$

The Slepian model at the upcrossing of level u by $E(t)$ is thus described by

$$\mathbf{Y}(t; u) = \mathbf{m}(t; u, \Theta, \dot{Z}) + \mathbf{E}_\theta(t),$$

where Θ is distributed uniformly on $[0, 2\pi)$, while \dot{Z} is independent of Θ and of residual process $\mathbf{E}_\theta(t)$, and \dot{Z} when divided by $2u\sqrt{\lambda_2(1-\rho^2)}$ has the Rayleigh distribution.

Assuming that δ in the proportion $\delta/(2\pi)$ of empty envelope excursions has been approximated by the excursion time of the regression process $\mathbf{m}(t; u, \Theta, \dot{Z})$ in the Slepian model, Ditlevson and Lindgren (1988) using Taylor expansions of this process have obtained

$$(8) \quad \frac{\nu_0^+(u)}{\nu^+(u)} \approx \int_{-u}^u \frac{\phi(\eta)}{\sqrt{1+\epsilon^2/4-\epsilon/2}} \left(1 - \sqrt{2\pi} \frac{\Phi\left(\gamma\pi \frac{u^2-\eta^2+\epsilon u\eta}{u} - \frac{1}{2}\right)}{\gamma\pi \frac{u^2-\eta^2+\epsilon u\eta}{u}} \right) d\eta,$$

where ϕ and Φ are the standard normal density and distribution function, respectively while $\epsilon = (\lambda_3 - 3\lambda_2\lambda_1 + 2\lambda_1^3)/(\lambda_2 - \lambda_1^2)^3/2$ is the skewness parameter of the spectrum. If the skewness is moderate, i.e. when we may assume that $\epsilon \approx 0$, then the formula takes a simpler

form

$$(9) \quad \frac{\nu_0^+(u)}{\nu^+(u)} \approx 2 \int_0^u \phi(\eta) \left(1 - \sqrt{2\pi} \frac{\Phi\left(\gamma\pi \frac{u^2 - \eta^2}{u} - \frac{1}{2}\right)}{\gamma\pi \frac{u^2 - \eta^2}{u}} \right) d\eta.$$

Further approximations can be obtained by Taylor expansions of the normal distribution function Φ .

4. ENVELOPE FIELD FOR SEA SURFACE

Sea surface. Throughout the paper we assume that the sea surface is modeled by a homogeneous Gaussian field defined uniquely by its (continuous) directional spectrum for which one can take, for example, a JONSWAP spectrum. A brief account of the terminology and notation for general Gaussian fields is given in Appendix A. In oceanography coordinates of $\boldsymbol{\tau}$ corresponds to spatial and temporal coordinates, i.e. $\boldsymbol{\tau} = (x, y, t)$, while for the sea surface instead of $X(\boldsymbol{\tau})$ we use the notation $W(x, y, t)$.

The problem with spectra for the sea surface is that they are degenerated in the full three dimensional space. This is due to the dispersion relation which reduce dimension of the spectral domain by one. Namely, the spectral measure σ is given by the unitary spectral density S through

$$\sigma(A) = \int_{-\infty}^{\infty} \int_{-\pi}^{\pi} \mathbf{1}_A(\boldsymbol{\lambda}(\omega, \theta)) \cdot S(\omega, \theta) d\omega d\theta,$$

where $\mathbf{1}_A(x) = 1$ if $x \in A$ and zero otherwise and the dispersion relation for deep waters is given by

$$\boldsymbol{\lambda}(\omega, \theta) = \left(\frac{\omega^2}{g} \cos \theta, \frac{\omega^2}{g} \sin \theta, \omega \right).$$

Here g is the gravity acceleration.

The symmetry relation $\sigma(\boldsymbol{\lambda}) = \sigma(-\boldsymbol{\lambda})$ translates to

$$(10) \quad S(T(\omega, \theta)) = S(\omega, \theta),$$

where

$$(11) \quad T(\omega, \theta) = \begin{cases} (-\omega, \theta - \pi) & \text{if } \theta \in [0, \pi], \\ (-\omega, \theta + \pi) & \text{if } \theta \in [-\pi, 0). \end{cases}$$

The above transformation can be interpreted more intuitively if we consider $\mathbb{R} \times (-\pi, \pi]$ as the union of two polar coordinate systems one corresponding to positive ω , $[0, \infty) \times (-\pi, \pi]$, and

other, the anti-system $(-\infty, 0] \times (-\pi, \pi]$, corresponding to negative ω . The transformation T takes a point from one system to the “anti-system” and then rotates it there by π .

Because of the symmetry relation (10) the unitary spectrum is uniquely related to the physical spectrum $\tilde{S}(\omega, \theta)$, $\omega > 0$, which is more frequently seen in engineering literature, by

$$\tilde{S}(\omega, \theta) = 2S(\omega, \theta), \omega > 0.$$

Further, the set Λ^+ described in Appendix A corresponds in the reduced domain to $\Gamma^+ = \boldsymbol{\lambda}^{-1}(\Lambda^+)$ and a choice of $\Lambda^+ \subseteq \mathbb{R}^3$ is equivalent to a choice of $\Gamma^+ \subset \mathbb{R} \times (-\pi, \pi]$ such that the intersection $T(\Gamma^+) \cap \Gamma^+$ has zero area (zero Lebesgue measure) and $T(\Gamma^+) \cup \Gamma^+ = \mathbb{R} \times (-\pi, \pi]$.

For the purpose of computations continuous models are typically approximated by their discretized versions. The general discrete model is defined in Example 1 of Appendix A. The discretized sea surface is obtained by taking atoms $\boldsymbol{\lambda}_j$ corresponding to the centers of cells ω_j and θ_j of a certain grid of $\mathbb{R} \times (-\pi, \pi]$ that is symmetric with respect to the transformation T . Then

$$\sigma(\boldsymbol{\lambda}_j) = S(\omega_j, \theta_j) \Delta\omega_j \Delta\theta_j,$$

where S is the unitary spectral density and $\Delta\omega_j$, $\Delta\theta_j$ are increments over a cell of the grid of ω 's and θ 's.

Versions of envelope field. Note that because of the symmetry of σ the statistical distributions of W (or its Hilbert transform when considered individually) do not depend on the choice of Λ^+ . However, one has to bear in mind that the choice of Λ^+ affects distributional properties of the envelope. For example, the values of spectral moments λ_{ijk} are affected by Λ^+ and, as a result, also the joint distributions of W , \hat{W} . In a given application it may be important to choose Λ^+ in such a way that the envelope process will possess natural or desirable properties. While in general there are infinitely many such choices some additional symmetries of random sea surface suggest the following “natural” one

$$(12) \quad \Lambda^+ = \{(x_1, x_2, x_3) \in \mathbb{R}^3 : x_3 \geq 0\}.$$

Following Appendix B the Hilbert transform of the discretized process W has the form

$$\hat{W}(\boldsymbol{\tau}) = \sum_{\boldsymbol{\lambda}_j \in \Lambda^+} \sqrt{2\sigma(\boldsymbol{\lambda}_j)} R_j \sin(\boldsymbol{\lambda}_j^T \boldsymbol{\tau} + \epsilon_j).$$

The Hilbert transform has the same unitary spectrum and thus the same distribution as the original field W . Also evaluated at the same fixed point (\mathbf{p}, t) the two random variables $W(\mathbf{p}, t)$ and $\hat{W}(\mathbf{p}, t)$ are independent. However stochastic fields W and \hat{W} are dependent. For example, the covariances between derivatives of W and \hat{W} are given through the spectral moments of W as, for example,

$$\text{Cov}(\hat{W}_x, W) = \lambda_{100} = -\text{Cov}(\hat{W}, W_x).$$

We have already remarked that these covariances are affected by a choice of Λ^+ and thus so is the dependence structure of W and \hat{W} .

The *real envelope process* $E(\mathbf{p}, t)$ is defined as

$$(13) \quad E(\boldsymbol{\tau}) = \sqrt{W(\boldsymbol{\tau})^2 + \hat{W}(\boldsymbol{\tau})^2},$$

or in the discretized version

$$E(\boldsymbol{\tau}) = \sqrt{\left[\sum_{\boldsymbol{\lambda}_j \in \Lambda^+} \sqrt{2\sigma(\boldsymbol{\lambda}_j)} R_j \cos(\boldsymbol{\lambda}_j^T \boldsymbol{\tau} + \epsilon_j) \right]^2 + \left[\sum_{\boldsymbol{\lambda}_j \in \Lambda^+} \sqrt{2\sigma(\boldsymbol{\lambda}_j)} R_j \sin(\boldsymbol{\lambda}_j^T \boldsymbol{\tau} + \epsilon_j) \right]^2}.$$

Note, that the envelope field is positive and always stays above the sea surface. It is also depending on a choice of Λ^+ because of the dependence between W and \hat{W} . The following two subsections illustrate importance of the choice of Λ^+ .

“Narrow-band” example. The following example is often used to illustrate the envelope for narrow band processes. Assume that Λ^+ contains only two atoms $\boldsymbol{\lambda} - \boldsymbol{\delta}$, $\boldsymbol{\lambda} + \boldsymbol{\delta}$ at which spectrum is defined as $\sigma(\boldsymbol{\lambda} - \boldsymbol{\delta}) = \sigma(\boldsymbol{\lambda} + \boldsymbol{\delta}) = 1/2$. We have

$$\begin{aligned} W(\boldsymbol{\tau}) &= R_1 \cos [(\boldsymbol{\lambda} + \boldsymbol{\delta})^T \boldsymbol{\tau} + \epsilon_1] + R_2 \cos [(\boldsymbol{\lambda} - \boldsymbol{\delta})^T \boldsymbol{\tau} + \epsilon_2] \\ &= 2R_1 \cos(\boldsymbol{\lambda}^T \boldsymbol{\tau} + \bar{\epsilon}) \cos(\boldsymbol{\delta}^T \boldsymbol{\tau} + \tilde{\epsilon}) + \\ &\quad + (R_2 - R_1) \cos [(\boldsymbol{\lambda} - \boldsymbol{\delta})^T \boldsymbol{\tau} + \epsilon_2] \\ \hat{W}(\boldsymbol{\tau}) &= R_1 \sin [(\boldsymbol{\lambda} + \boldsymbol{\delta})^T \boldsymbol{\tau} + \epsilon_1] + R_2 \sin [(\boldsymbol{\lambda} - \boldsymbol{\delta})^T \boldsymbol{\tau} + \epsilon_2] \\ E(\boldsymbol{\tau}) &= \sqrt{(R_1 - R_2)^2 + 4R_1 R_2 \cos^2(\boldsymbol{\delta}^T \boldsymbol{\tau} + \tilde{\epsilon})}, \end{aligned}$$

where $\bar{\epsilon} = (\epsilon_1 + \epsilon_2)/2$ and $\tilde{\epsilon} = (\epsilon_1 - \epsilon_2)/2$.

Since $|R_1 - R_2|$ is small relatively to R_1 with large probability, we often observe

$$(14) \quad W(\boldsymbol{\tau}) \approx 2R_1 \cos(\boldsymbol{\lambda}^T \boldsymbol{\tau} + \bar{\epsilon}) \cos(\boldsymbol{\delta}^T \boldsymbol{\tau} + \tilde{\epsilon})$$

$$(15) \quad E(\boldsymbol{\tau}) \approx 2R_1 |\cos(\boldsymbol{\delta}^T \boldsymbol{\tau} + \tilde{\epsilon})|.$$

It is easy to calculate that the squared correlation between the x -derivatives of the process and its Hilbert transform is $\rho^2 = \frac{1}{1+\delta_1^2/\lambda_1^2}$.

If we assume that $|\boldsymbol{\delta}|$ is essentially smaller than $|\boldsymbol{\lambda}|$, then the signal $W(\boldsymbol{\tau})$ is a cosine wave corresponding to the high frequency $|\boldsymbol{\lambda}|$, modulated by a cosine amplitude having the low frequency $|\boldsymbol{\delta}|$. If the atoms are on the horizontal axis, i.e. $\boldsymbol{\lambda} = (\lambda_1, 0, 0)$ and $\boldsymbol{\delta} = (\delta_1, 0, 0)$, then this ‘‘narrow band’’ case results in $\rho^2 \approx 1$. We see that the envelope coincides with the low frequency varying amplitude. This simple example illustrates the usual interpretation of the envelope as a process which is governing slow frequency modulation of amplitudes of high frequency components in the signal.

We conclude this example with analysis what can happen if we choose a different version of the envelope. Clearly, for the two atoms $\boldsymbol{\lambda} - \boldsymbol{\delta}$, $\boldsymbol{\lambda} + \boldsymbol{\delta}$, in the full spectral domain there exist the two ‘‘anti-atoms’’ $\boldsymbol{\delta} - \boldsymbol{\lambda}$, $-\boldsymbol{\lambda} - \boldsymbol{\delta}$, and we can choose Λ^+ in such a way that now $\boldsymbol{\delta} - \boldsymbol{\lambda}$, $\boldsymbol{\lambda} + \boldsymbol{\delta}$ belong to it. It is easy to notice that this time $\rho^2 = \frac{1}{1+\lambda_1^2/\delta_1^2}$. Under the assumption that $|\boldsymbol{\delta}|$ is relatively small as compared to $|\boldsymbol{\lambda}|$ we obtain in this ‘‘narrow band’’ case and for atoms on the horizontal axis $\rho^2 \ll 1$ as it would be for the ‘‘broad band’’ case with the original choice of Λ^+ . Moreover the rest of the above discussion of the envelope remains valid except that now we switch $\boldsymbol{\delta}$ with $\boldsymbol{\lambda}$. Consequently, now the envelope will be modulated by high frequency $|\boldsymbol{\lambda}|$ and thus its usual interpretation as the low frequency component fails completely. We also note that this envelope would result in a higher rate of empty excursions as compared with the previous choice of Λ^+ (see Figure 3).

Crossings intensity in the principal wave direction. Let us consider the intensity of up-crossings of a u -level by the envelope in the direction $y = 0$. We note that the intensity crossing is dependent on a chosen direction on the plane although we will not indicate it in

our notation and thus we will “reuse” the notation $\nu^+(u)$ for this intensity. Thus

$$\begin{aligned}\nu^+(u) &= \mathbf{E}(E_x^+(\mathbf{0})|E(\mathbf{0}) = u) \cdot \frac{u}{\lambda_{000}} e^{-\frac{u^2}{2\lambda_{000}}}, \\ &= \sqrt{\frac{\lambda_{200}}{2\pi}} \sqrt{1 - \rho^2} \cdot \frac{u}{\lambda_{000}} e^{-\frac{u^2}{2\lambda_{000}}}, \quad u > 0,\end{aligned}$$

where $\rho^2 = \lambda_{100}^2/(\lambda_{000}\lambda_{200})$ [see also Lindgren (1989)]. The highest intensity is reached for the level $u = \sqrt{\lambda_{000}}$ often called the reference level for the envelope, and is equal

$$\nu_{max}^+ = \sqrt{\frac{\lambda_{200}}{2\pi \cdot e \cdot \lambda_{000}}} \sqrt{1 - \rho^2}.$$

We observe that the intensity of envelope crossing in the direction $y = 0$ depends on the choice of Λ^+ only through λ_{100} and in such a way that larger $|\lambda_{100}|$ (larger the squared correlation ρ^2) corresponds to lower crossing intensity. If one is interested in an envelope that is smoother than the sea surface and following closer to the local extremes, then a reasonable choice of Λ^+ is the one that minimizes crossing intensity and thus maximizes the spectral functional

$$\lambda_{100} = 2 \int_{\Lambda^+} \lambda_1 d\sigma(\boldsymbol{\lambda}) = 2 \int_{\Gamma^+} \frac{\omega^2}{g} \cos \theta \cdot S(\omega, \theta) d\omega d\theta.$$

Clearly, the choice will depend on the form of a spectrum in hand. For example, consider a spectrum having symmetry properties similar to these exhibited in Figure 1 (right) by the JONSWAP spectrum used in the examples. Considering the symmetry given by (10), it is rather obvious that the choice of $\Gamma^+ = \{(\omega, \theta) : \theta \in (-\frac{\pi}{2}, \frac{\pi}{2}], \omega \in \mathbb{R}\}$ is the optimal in such a situation.

For comparison, the natural choice corresponding to (12), i.e. taking $\Gamma^+ = \{(\omega, \theta) : \theta \in (-\pi, \pi), \omega > 0\}$ will result in λ_{100} smaller by

$$-4 \int_{\omega > 0} \int_{\theta \in (-\pi, -\pi/2] \cup (\pi/2, \pi]} \frac{\omega^2}{g} \cos \theta \cdot S(\omega, \theta) d\omega d\theta.$$

This is essentially negligible if we deal with directional spectra obtained by quickly vanishing spreading functions, since such spectra are, for all practical purposes, equal to zero for $\theta \in (-\pi, -\pi/2] \cup (\pi/2, \pi]$. However this condition will no longer be true if, for example, there will be an additional swell portion of the spectrum corresponding to these values of azimuth θ .

TABLE 1. VERSIONS OF ENVELOPE IN TERMS OF Λ^+ and Γ^+ .

Λ^+	Γ^+	Comment
$x_1 > 0$	$\theta \in (-\frac{\pi}{2}, \frac{\pi}{2}]$	Maximizes ρ^2 , minimizes crossing intensity
$x_2 > 0$	$\theta \in (0, \pi]$	Maximizes crossing intensity, $\rho^2 = 0$
$x_3 > 0$	$\omega > 0$	Natural choice for the sea surface.

Finally, consider $\Lambda^+ = \{(x_1, x_2, x_3), x_2 \geq 0\}$. If spectrum S is symmetric with respect to θ , then λ_{100} is equal to zero. Thus the maximal intensity of envelope crossings (at level $\sqrt{\lambda_{000}}$) is equal to $\sqrt{\frac{1}{2\pi e}} \sqrt{\lambda_{200}/\lambda_{000}}$. For comparison, the intensity crossing of the sea surface at the reference level zero is given by $\frac{1}{2\pi} \sqrt{\lambda_{200}/\lambda_{000}}$, thus the ratio of these intensities is equal to $\sqrt{2\pi/e} \approx 1.52$. This envelope no longer represents wave groups because by our definitions there would be 50% more wave groups than waves. Recall also that ρ represents correlation of the derivative of process with its Hilbert transform and thus in this case the envelope will no longer follow the extrema of the process. We conclude that such a choice of Λ^+ does not carry with itself properties that are typically attributed to the envelope.

5. DISTRIBUTIONS OF WAVE AND ENVELOPE VELOCITIES

In this section we show how the theory of sampling distributions based on a generalized Rice formula can be utilized to compute the velocity distributions for waves and waves groups that are represented here by the envelope field.

In the simple ‘‘narrow band’’ example, where the relations (14) and (15) were found, the velocities are easy to define. In the special case $\boldsymbol{\lambda} - \boldsymbol{\delta} = (\omega_1^2/g, 0, \omega_1)$ and $\boldsymbol{\lambda} + \boldsymbol{\delta} = (\omega_2^2/g, 0, \omega_2)$, where $\omega_1 = \omega - \delta$ and $\omega_2 = \omega + \delta$ for some $\delta > 0$ and using the approximation (14) we obtain that the high frequency modulation speed, i.e. the speed of individual waves, is given by

$$V_W = g \frac{\omega}{\omega^2 + \delta^2},$$

while by (15) the envelope is propagating with the speed

$$V = g \frac{1}{2\omega}.$$

This illustrative example demonstrates that the speed ratio $V_W/V = \frac{2}{1+\delta^2/\omega^2} < 2$ and is approximately equal to 2 if $\delta^2 \ll \omega^2$. In order to extend this result to the velocities for

more general spectra such as, for example, JONSWAP spectra, one needs to formally define the velocities for moving surfaces and then analyze their statistical distributions using, for example, Rice's formula.

There is a variety of ways to introduce velocity for dynamically changing surface [see Baxevani et al. (2003)]. Here for simplicity we focus on the velocity describing the motion of a contour level in the specified direction given by an azimuth α . We define this velocity by the equations

$$(16) \quad \begin{bmatrix} E_x & E_y \\ -\sin \alpha & \cos \alpha \end{bmatrix} \mathbf{V}_\alpha = - \begin{bmatrix} E_t \\ 0 \end{bmatrix},$$

where the first equation in the system guarantees that the motion following \mathbf{V}_α stays on the same envelope level and in this sense describes motion of the constant level contours, while the second equation implies that the velocity points always in the direction α . If α is constant, then the motion is along a straight line. Further assume that $\alpha = 0$, i.e. that we are interested in the constant direction coinciding with the principle direction of waves. It follows from (16) and (13) that the velocity $\mathbf{V}_0 = (V, 0)$ is given by

$$(17) \quad V = - \frac{W_t \cdot W + \hat{W}_t \cdot \hat{W}}{W_x \cdot W + \hat{W}_x \cdot \hat{W}}.$$

Here we obtain the statistical sampling distributions of the velocity V for general spectra and discuss how they are influenced by different sampling schemes. Three cases are considered:

- a) unbiased sampling,
- b) sampling at the points of u -level crossings of the envelope field crosssection in the principal wave direction, i.e. at the crossings of $E(x, 0, 0)$,
- c) sampling at the u -level crossings contours of the envelope field, i.e. at the countours of $E(x, y, 0)$.

Let us define $\mathcal{C}_u^0 = \{x \in \mathbb{R} : E(x, 0, 0) = u\}$ and $\mathcal{C}_u^1 = \{(x, y) \in \mathbb{R}^2 : E(x, y, 0) = u\}$. It follows from the generalization of Rice's formula presented in (2) that the distributions in

b) and c) are different and given by

$$\begin{aligned} \mathbb{P}\left(V(x, 0, 0) \in A \mid x \in \mathcal{C}_u^0\right) &= \frac{\mathbb{E}\left(\left\{-\frac{W_t \cdot W + \hat{W}_t \cdot \hat{W}}{W_x \cdot W + \hat{W}_x \cdot \hat{W}} \in A\right\} E_x \mid E = u\right)}{\mathbb{E}\left(E_x \mid E = u\right)}, \\ \mathbb{P}\left(V(x, y, 0) \in A \mid (x, y) \in \mathcal{C}_u^1\right) &= \frac{\mathbb{E}\left(\left\{-\frac{W_t \cdot W + \hat{W}_t \cdot \hat{W}}{W_x \cdot W + \hat{W}_x \cdot \hat{W}} \in A\right\} \sqrt{E_x^2 + E_y^2} \mid E = u\right)}{\mathbb{E}\left(\sqrt{E_x^2 + E_y^2} \mid E = u\right)}. \end{aligned}$$

Note that the above distributions are expressed in the terms of complex functions of multi-dimensional Gaussian vectors with coordinates $W, \hat{W}, W_t, \hat{W}_t, W_x, \hat{W}_x$ in the cases a), b) and additionally W_y, \hat{W}_y in the case c). However straightforward although tedious calculations [see Appendix C and Baxevani et al. (2003)] lead to the following general template for the considered envelope velocity distributions

$$(18) \quad -\frac{1}{a} \left(b + \sqrt{a \cdot c - b^2} \cdot \frac{X}{Y} \right),$$

where the constants are given by

$$\begin{aligned} a &= \lambda_{200}(1 - \rho^2), \\ b &= \lambda_{101} - \lambda_{100}\lambda_{001}/\lambda_{000}, \\ c &= \lambda_{002} - \lambda_{001}^2/\lambda_{000}, \end{aligned}$$

and variables X and Y are independent, X having the standard normal distribution while the distribution of Y is

- a) the standard normal,
- b) the Rayleigh distribution,
- c) given by a complex but explicit density that is expressed in (27) of Appendix C by the means of Bessel functions.

In the above, λ_{ijk} are spectral moments of $W(\mathbf{p}, t)$ as defined by (21) in Appendix A. Additionally for the part c) it assumed (as in all our examples) that the directional spectrum is symmetric with respect to the principal wave direction and thus $\lambda_{010} = \lambda_{011} = \lambda_{110} = 0$.

For comparison, the velocity of the sea surface has the same template (18) but with the constants $a = \lambda_{200}$, $b = \lambda_{101}$, and $c = \lambda_{002}$. Notice that for JONSWAP spectra and for the second choice in Table 1 ($\lambda_{100} = 0$) the template constants a and b for the waves coincide with the ones for the envelope. Thus statistically velocities of the envelope and of individual

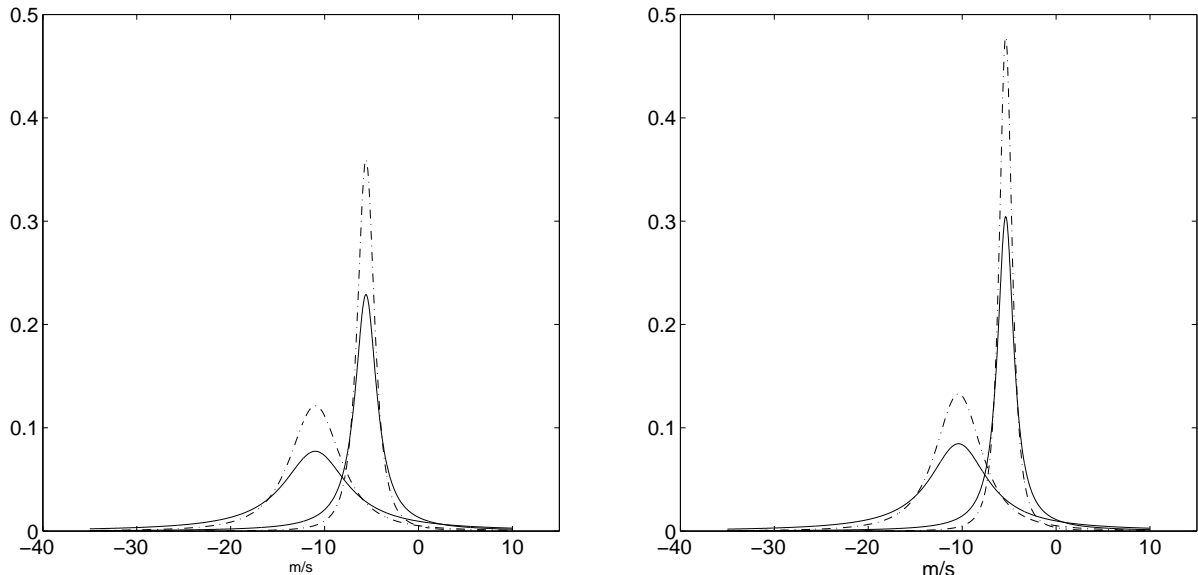


FIGURE 4. Distributions of velocities in the direction $y = 0$ for envelope field and sea surface sampled at: the contours (left); and the crossing points along $y = 0$ (right).

waves are centered at the same values which again demonstrates how counterintuitive things can go for certain choices of the envelope.

It is interesting that the considered velocity under the both biased sampling distributions on u -level contours does not depend on the level u , i.e. they are the same independently of the elevation at which the velocity is measured.

6. EXAMPLES

In this section we consider the directional Gaussian sea surface obtained from the JONSWAP spectrum $\tilde{S}(\omega, \theta) = S(\omega)D(\omega, \theta)$, where

$$S(\omega) = g^2 \frac{\alpha}{\omega^5} e^{-1.25\omega_p^4/\omega^4} \rho^{\psi(\omega)},$$

with $\psi(\omega) = e^{-(\omega-\omega_p)^2/(2\sigma^2\omega_p^2)}$, where σ is a jump function of ω :

$$\sigma = \begin{cases} 0.07 & \text{if } \omega/\omega_p \leq 1, \\ 0.09 & \text{if } \omega/\omega_p > 1. \end{cases}$$

and α is a scale, ρ controls the shape, and ω_p is the peak frequency. The spreading function is given by $D(\omega, \theta) = G_0 \cos^{2c}(\theta/2)$. The alternative data driven parameters can be introduced

by the relations [see Goda (1990)]:

$$\alpha = \beta_J H_{1/3}^2 \omega_p^4,$$

$$\beta_J = \frac{0.06238(1.094 - 0.01915 \log \rho)}{0.23 + 0.0336\rho - 0.185(1.9 + \rho)^{-1}},$$

$$\omega_p = 2\pi \frac{1 - 0.132(\rho + 0.2)^{-0.559}}{T_{1/3}},$$

where $H_{1/3}$ is the significant waves height, $T_{1/3}$ their average period. The following values of the parameters were assumed in the computed examples: $H_{1/3} = 7[m]$, the peak period $2\pi/\omega_p = 11[s]$, $\rho = 2.3853$, $c = 15$. The spectrum is shown in Figure 1 (right). For the envelope we have chosen Λ^+ given in (12) which corresponds to $\Gamma^+ = [0, \infty) \times (-\pi, \pi]$.

In Figure 4 (left), we present the unbiased and biased sampling distributions of velocities both for the envelope and for the sea surface. The solid lines represent the unbiased densities and the dashed-dotted ones corresponds to the biased sampling densities. We see that the biased sampling distribution which are more important for applications, are more concentrated around its center. The group velocity is smaller than that of individual waves as it is observed in the real life records. The peaks are at $-5.58[m/s]$ and $-10.98[m/s]$. Thus waves are roughly twice as fast as groups, the result in agreement with conclusions of the “narrow banded” example.

CONCLUSION

It is important to realize that even for studying the statistical properties of sea *surface*, i.e. of $W(x, y, t)$, in the direction along $y = 0$ the envelope *field* $E(x, y, t)$ is a different concept from the envelope process defined for one dimensional record $W(x, 0, t)$, the latter often used in ocean engineering for analysis of wave movements. Moreover, even studying the envelope field along the line $y = 0$ leads to different sampling distributions than studying it along the crossing contours. It shown in our computations of the distribution of velocities for the classical one dimensional envelope and in our case the resulting distributions are presented in Figure 4 (right). As we can observe, the distributions are not identical, the one dimensional record distributions are slightly more peaky.

We have seen that from the formal point of view the multidimensional envelope is not essentially harder to study than its one-dimensional counterpart. Thus for the sea surface

which is a three dimensional field, it is more appropriate but also manageable to study effectively such “fully” dimensional objects and concepts as wave contours, envelope contours, or vector velocities. In this work we demonstrate this for few simple examples. Through similar approach one can tackle many other important “multidimensional” problems.

APPENDIX A. GAUSSIAN FIELDS

Here we present some basic definitions and properties for the Gaussian sea model (for more details see Baxevani et al. (2003) and references therein). Let $\{X(\boldsymbol{\tau})\}_{\boldsymbol{\tau} \in \mathbb{R}^3}$ be a stationary Gaussian field, where $\boldsymbol{\tau} = (\mathbf{p}, t) = (x, y, t)$ is a point in \mathbb{R}^3 . The covariance function $R(\boldsymbol{\tau}) = \text{Cov}(X_{\boldsymbol{\tau}_0 + \boldsymbol{\tau}}, X_{\boldsymbol{\tau}_0})$ can be written in the form

$$(19) \quad R(\boldsymbol{\tau}) = \int_{\mathbb{R}^3} \exp(i\boldsymbol{\lambda}^T \boldsymbol{\tau}) d\sigma(\boldsymbol{\lambda}),$$

where $\sigma(\boldsymbol{\lambda})$ is a finite measure on Borel sets of \mathbb{R}^3 called the *spectral measure* of $X(\boldsymbol{\tau})$.

The process $X(\boldsymbol{\tau})$ has the following spectral representation

$$(20) \quad X(\boldsymbol{\tau}) = \int_{\mathbb{R}^3} \exp(i\boldsymbol{\lambda}^T \boldsymbol{\tau}) d\zeta(\boldsymbol{\lambda}),$$

where the process $\zeta(\boldsymbol{\lambda})$ is complex valued with zero mean, orthogonal increments, and such that $E(|\zeta(\boldsymbol{\lambda})|^2) = \sigma(-\infty, \boldsymbol{\lambda}]$. Additionally, since $X(\boldsymbol{\tau})$ is real, we have the following symmetry $\zeta(A) = \overline{\zeta(-A)}$. Therefore it is often more convenient to represent the process and its covariance as follows

$$\begin{aligned} X(\boldsymbol{\tau}) &= 2\Re \left(\int_{\Lambda^+} \cos(\boldsymbol{\lambda}^T \boldsymbol{\tau}) d\zeta(\boldsymbol{\lambda}) \right) - \zeta(\{0\}), \\ R(\boldsymbol{\tau}) &= 2 \int_{\Lambda^+} \cos(\boldsymbol{\lambda}^T \boldsymbol{\tau}) d\sigma(\boldsymbol{\lambda}) - \sigma(\{0\}). \end{aligned}$$

where Λ^+ is any set in \mathbb{R}^3 such that $-\Lambda^+ \cap \Lambda^+ = \{0\}$ and $-\Lambda^+ \cup \Lambda^+ = \mathbb{R}^3$. An example of such a set is

$$\Lambda^+ = \{(x_1, x_2, x_3) \in \mathbb{R}^3 : x_3 > 0\} \cup \{(x_1, x_2, 0) \in \mathbb{R}^3 : x_2 > 0\} \cup \{(x_1, 0, 0) \in \mathbb{R}^3 : x_1 \geq 0\}.$$

When selecting Λ^+ it is often more convenient to consider a weaker but sufficient condition

$$\sigma(-\Lambda^+ \cap \Lambda^+) = 0.$$

The *spectral moments* λ_{ijk} , if they are finite, are defined as

$$(21) \quad \lambda_{ijk} = 2 \int_{\Lambda^+} \lambda_1^i \lambda_2^j \lambda_3^k d\sigma(\boldsymbol{\lambda}),$$

where $\boldsymbol{\lambda} = (\lambda_1, \lambda_2, \lambda_3)$. The variance of the field can be expressed in terms of spectral moments as the zero moment λ_{000} decreased by the weight $\sigma(\mathbf{0})$ of the spectral measure at zero. If $i+j+k$ is even, then λ_{ijk} does not depend on a choice of Λ^+ because of the symmetry of σ . However for odd $i+j+k$, different Λ^+ can, in general, lead to different λ_{ijk} which is important when the distribution of the envelope field is discussed.

Example 1. Assume that the spectral measure σ is discrete, i.e. has discrete support at points $\{\boldsymbol{\lambda}_j\} = \{(\lambda_{1j}, \lambda_{2j}, \lambda_{3j})\}$, $j \in \mathbb{N}$, of which none is equal to zero, with masses $\sigma(\boldsymbol{\lambda}_j)$. For a real valued random field the support of σ has to be symmetric, i.e. if $\boldsymbol{\lambda}_j$ is in the support, then also $-\boldsymbol{\lambda}_j$ is in the support and both frequencies have equal masses $\sigma(\boldsymbol{\lambda}_j) = \sigma(-\boldsymbol{\lambda}_j)$. It follows directly from the spectral representation (20) that

$$X(\boldsymbol{\tau}) = \sum_{\boldsymbol{\lambda}_j \in \Lambda^+} \sqrt{2\sigma(\boldsymbol{\lambda}_j)} R_j \cos(\boldsymbol{\lambda}_j^T \boldsymbol{\tau} + \epsilon_j).$$

Here (R_j) and (ϵ_j) are two independent sequences of independent identically distributed random variables, the first one distributed according to the Rayleigh density

$$(22) \quad f(r) = r e^{-r^2/2}, \quad r > 0$$

and the second one distributed uniformly on $[0, 2\pi]$.

If none of $\boldsymbol{\lambda}_j$'s is not on the line $x_3 = 0$, one possible choice for Λ^+ is

$$\Lambda^+ = \{(x_1, x_2, x_3) \in \mathbb{R}^3 : x_3 \geq 0\}.$$

By (19), the covariance of this field is a sum of cosines

$$R(\boldsymbol{\tau}) = \sum_{\boldsymbol{\lambda}_j \in \mathbb{R}^3} \sigma(\boldsymbol{\lambda}_j) \cos(\boldsymbol{\lambda}_j^T \boldsymbol{\tau}) = 2 \sum_{\boldsymbol{\lambda}_j \in \Lambda^+} \sigma(\boldsymbol{\lambda}_j) \cos(\boldsymbol{\lambda}_j^T \boldsymbol{\tau}).$$

Example 2. If the covariance function $R(\boldsymbol{\tau})$ decreases sufficiently fast at infinity, so that $\int_{\mathbb{R}^3} |R(\boldsymbol{\tau})| d\boldsymbol{\tau} < \infty$, then σ has a density $S(\boldsymbol{\lambda})$ and the covariance function can be represented as its Fourier integral

$$(23) \quad R(\boldsymbol{\tau}) = \int_{\mathbb{R}^3} \exp(i\boldsymbol{\lambda}^T \boldsymbol{\tau}) S(\boldsymbol{\lambda}) d\boldsymbol{\lambda}.$$

The spectral density $S(\boldsymbol{\lambda})$ is real, non-negative, bounded and symmetric, i.e. $S(\boldsymbol{\lambda}) = S(-\boldsymbol{\lambda})$ for all $\boldsymbol{\lambda} \in \mathbb{R}^3$. In this case it is sufficient to consider Λ^+ that has zero volume (zero Lebesgue measure) when intersected with $-\Lambda^+$.

APPENDIX B. ENVELOPE FIELD

In this appendix we discuss the envelope field following Adler (1978). Let $X(\boldsymbol{\tau})$ have a representation given by (20). We define a stochastic measure

$$\hat{\zeta}(A) = -i\zeta(A \cap \Lambda^+) + \zeta(A \cap \{\mathbf{0}\}) + i\zeta(A \cap -\Lambda^+),$$

where Λ^+ is as discussed in the previous appendix.

Note $\text{Var}\hat{\zeta}(A) = \text{Var}\zeta(A) = \sigma(A)$. Thus the process defined by

$$\hat{X}(\boldsymbol{\tau}) = \int_{\mathbb{R}^3} \exp(i\boldsymbol{\lambda}^T \boldsymbol{\tau}) d\hat{\zeta}(\boldsymbol{\lambda})$$

has the same covariance function as $X(\boldsymbol{\tau})$. In the Gaussian case they have the same distributions. Moreover, $\hat{\zeta}$ satisfies the symmetry $\hat{\zeta}(A) = \overline{\hat{\zeta}(-A)}$ and thus $\hat{X}(\boldsymbol{\tau})$ is also a real process.

Let $X_H(\boldsymbol{\tau}) = \hat{X}(\boldsymbol{\tau}) - \zeta(\{\mathbf{0}\})$. The complex envelope process $\mathcal{E}(\boldsymbol{\tau})$ is defined by

$$\mathcal{E}(\boldsymbol{\tau}) = X(\boldsymbol{\tau}) + iX_H(\boldsymbol{\tau}),$$

and the (real) envelope process is defined by

$$E(\boldsymbol{\tau}) = |\mathcal{E}(\boldsymbol{\tau})| = \sqrt{X^2(\boldsymbol{\tau}) + X_H^2(\boldsymbol{\tau})}.$$

To study statistical distributions of the envelopes the covariances between processes $X(\boldsymbol{\tau})$, $\hat{X}(\boldsymbol{\tau})$ and their derivatives have to be computed. The following simple property can be conveniently utilized for this purpose. Let complex functions $f(\boldsymbol{\lambda})$, $g(\boldsymbol{\lambda})$ be square integrable with respect to $\sigma(\cdot)$. Define

$$\hat{f}(\boldsymbol{\lambda}) = \begin{cases} -i \cdot f(\boldsymbol{\lambda}) & : \boldsymbol{\lambda} \in \Lambda^+, \\ f(\mathbf{0}) & : \boldsymbol{\lambda} = \mathbf{0}, \\ i \cdot f(\boldsymbol{\lambda}) & : \boldsymbol{\lambda} \in -\Lambda^+. \end{cases}$$

Then

$$\int f(\boldsymbol{\lambda}) d\hat{\zeta}(\boldsymbol{\lambda}) = \int \hat{f}(\boldsymbol{\lambda}) d\zeta(\boldsymbol{\lambda})$$

and

$$\text{Cov} \left[\int f(\boldsymbol{\lambda}) d\hat{\zeta}(\boldsymbol{\lambda}), \int g(\boldsymbol{\lambda}) d\zeta(\boldsymbol{\lambda}) \right] = \int \hat{f}(\boldsymbol{\lambda}) \bar{g}(\boldsymbol{\lambda}) d\sigma(\boldsymbol{\lambda}).$$

The two-dimensional process $\mathbf{Y}(\boldsymbol{\tau}) = (X(\boldsymbol{\tau}), \hat{X}(\boldsymbol{\tau}))$ is a jointly stationary Gaussian vector process such that

$$\text{Cov} \left[\hat{X}(\boldsymbol{\nu} + \boldsymbol{\tau}), X(\boldsymbol{\nu}) \right] = \sigma(\{\mathbf{0}\}) - 2 \int_{\Lambda^+} \sin(\boldsymbol{\lambda}^T \boldsymbol{\tau}) d\sigma(\boldsymbol{\lambda}).$$

In a similar manner one can obtain the covariances between the derivatives. For example,

$$\text{Cov} \left[\frac{\partial \hat{X}}{\partial \tau_1}(\boldsymbol{\tau}), X(\boldsymbol{\tau}) \right] = 2 \int_{\Lambda^+} \lambda_1 d\sigma(\boldsymbol{\lambda}) = \lambda_{100} = -\text{Cov} \left[\hat{X}(\boldsymbol{\tau}), \frac{\partial X}{\partial \tau_1}(\boldsymbol{\tau}) \right].$$

APPENDIX C. GENERALIZED RICE FORMULA AND SAMPLING DISTRIBUTIONS

In the following a sketch of the argument for the generalized Rice formula as given in (5) is presented. We start with recalling the notion of generalized determinant that is used in the formulations of multivariate Rice formulas.

The generalized determinant is a standard concept in the algebraic setup. Here, we present it in a manner mostly convenient for the discussion of the generalized Rice formula. Let \mathbf{A} be a matrix mapping \mathbb{R}^k onto \mathbb{R}^n , where we assume $n \leq k$. Let $\mathcal{N} = \{\boldsymbol{\tau} : \mathbf{A}\boldsymbol{\tau} = \mathbf{0}\}$. The space \mathbb{R}^k has the following orthogonal decomposition

$$\mathbb{R}^k = \mathcal{N} + \mathcal{N}^\perp.$$

The dimensions of \mathcal{N} and \mathcal{N}^\perp are $k - n$ and n , respectively. The matrix \mathbf{A} restricted to \mathcal{N}^\perp can be viewed as a non-singular linear mapping from the n dimensional space \mathcal{N}^\perp to \mathbb{R}^n . Consider the $n \times n$ matrix $\mathbf{A}_{\mathcal{N}^\perp}$ of this restriction of \mathbf{A} in an arbitrary orthogonal basis in \mathcal{N}^\perp . The regular determinant $\det \mathbf{A}_{\mathcal{N}^\perp}$ is uniquely defined except for the sign. The positive generalized determinant of \mathbf{A} is defined as $\det \mathbf{A} = |\det \mathbf{A}_{\mathcal{N}^\perp}|$. In this paper, for the clarity of notation, $\det \mathbf{A}$ is often written as $\det(\mathbf{A})$.

The generalized determinant can be computed using methods for computing the regular determinant in terms of the following formula

$$\det \mathbf{A} = \sqrt{\det \mathbf{A}\mathbf{A}^T}.$$

Consider a set E of full volume in \mathcal{N}^\perp . Then the matrix \mathbf{A} transforms it to the full volume set $\mathbf{A}E$ in \mathbb{R}^n . The generalized determinant is equal to the proportion of the volumes of these two sets

$$\det \mathbf{A} = \mathcal{V}_n(\mathbf{A}E)/\mathcal{V}_n(E),$$

where \mathcal{V}_n stands for the relative volume of dimension n in the underlying linear space.

If we take the orthogonal sum $F = E + C$ of two sets $E \subseteq \mathcal{N}^\perp$ and $C \subseteq \mathcal{N}$, then $\mathcal{V}_k(F) = \mathcal{V}_n(E) \cdot \mathcal{V}_{k-n}(C)$. Consequently, for each set C in \mathcal{N} , we have

$$(24) \quad \mathcal{V}_{n-k}(C) = \det \mathbf{A} \cdot \frac{\mathcal{V}_k(F)}{\mathcal{V}_n(\mathbf{A}E)} = \det \mathbf{A} \cdot \frac{\mathcal{V}_k(F)}{\mathcal{V}_n(\mathbf{A}F)}.$$

For a vector \mathbf{x} , let $|\mathbf{x}|_m$ stand for the maximal absolute value of the coordinates of \mathbf{x} . Considering $\mathbf{A} = \dot{\mathbf{X}}(\boldsymbol{\tau}_0)$, $\epsilon > 0$, $C \subset \mathcal{N}$, and $E = \{\boldsymbol{\tau} \in [0, 1]^k : |\dot{\mathbf{X}}(\boldsymbol{\tau}_0)\boldsymbol{\tau}|_m < \epsilon/2\}$, equation (24) can be written as

$$\mathcal{V}_{n-k}(C) = \det \dot{\mathbf{X}}(\boldsymbol{\tau}_0) \cdot \frac{\mathcal{V}_k(F)}{\epsilon^n}.$$

Let $\mathcal{C} = \{\boldsymbol{\tau} \in [0, 1]^k : \mathbf{X}(\boldsymbol{\tau}) = \mathbf{u}_0\}$. For small $\epsilon > 0$, one can find the points $\boldsymbol{\tau}_i^\epsilon$, $i = 1, \dots, N_\epsilon$ on the contour \mathcal{C} such that the set $\{\boldsymbol{\tau} \in [0, 1]^k : |\mathbf{X}(\boldsymbol{\tau}) - \mathbf{u}_0|_m < \epsilon/2\}$ is closely approximated by $F_\epsilon = \bigcup_{i=1}^{N_\epsilon} F_i$, where

$$F_i = \{\boldsymbol{\tau} \in [0, 1]^k : |\dot{\mathbf{X}}(\boldsymbol{\tau}_i)(\boldsymbol{\tau} - \boldsymbol{\tau}_i)|_m < \epsilon/2\}.$$

(The sets are approximated by each other, in the sense that their symmetric difference has the volume converging to zero when ϵ converges to zero.)

Clearly, each F_i can be orthogonally decomposed around $\boldsymbol{\tau}_i$ into $F_i = E_i + C_i$ as discussed above. Then, for small ϵ , the pieces $\mathcal{C}_i = \mathcal{C} \cap F_i$ of the contour \mathcal{C} can be linearly approximated by C_i 's so that

$$\mathcal{V}_{n-k}(\mathcal{C}_i) \approx \mathcal{V}_{n-k}(C_i) = \det \dot{\mathbf{X}}(\boldsymbol{\tau}_i^\epsilon) \cdot \frac{\mathcal{V}_k(F_i)}{\epsilon^n}.$$

For $\epsilon > 0$ small enough and for $\boldsymbol{\tau} \in F_i$, one can approximate $\dot{\mathbf{X}}(\boldsymbol{\tau})$ by $\dot{\mathbf{X}}(\boldsymbol{\tau}_i^\epsilon)$. Thus

$$\begin{aligned} \mathcal{V}_{n-k}(\mathcal{C}) &= \sum_{i=1}^{N_\epsilon} \mathcal{V}_{n-k}(\mathcal{C}_i) \approx \sum_{i=1}^{N_\epsilon} \mathcal{V}_{n-k}(C_i) \\ &= \sum_{i=1}^{N_\epsilon} \det \dot{\mathbf{X}}(\boldsymbol{\tau}_i^\epsilon) \cdot \frac{\mathcal{V}_k(F_i)}{\epsilon^n} = \frac{1}{\epsilon^n} \sum_{i=1}^{N_\epsilon} \int_{F_i} \det \dot{\mathbf{X}}(\boldsymbol{\tau}_i^\epsilon) d\boldsymbol{\tau} \\ &\approx \frac{1}{\epsilon^n} \sum_{i=1}^{N_\epsilon} \int_{F_i} \det \dot{\mathbf{X}}(\boldsymbol{\tau}) d\boldsymbol{\tau} \approx \frac{1}{\epsilon^n} \int_{F_\epsilon} \det \dot{\mathbf{X}}(\boldsymbol{\tau}) d\boldsymbol{\tau} \\ &\approx \frac{1}{\epsilon^n} \int_{\{\boldsymbol{\tau} \in [0,1]^k: |\mathbf{X}(\boldsymbol{\tau}) - \mathbf{u}_0|_m < \epsilon/2\}} \det \dot{\mathbf{X}}(\boldsymbol{\tau}) d\boldsymbol{\tau}. \end{aligned}$$

Assuming that $\mathbf{X}(\boldsymbol{\tau})$ has the density $f_{\mathbf{X}(\boldsymbol{\tau})}(\mathbf{x})$, taking expectations from both sides of the above approximation and by letting ϵ converge to zero we obtain a multivariate version of Rice's formula

$$\begin{aligned} \mathbb{E}(\mathcal{V}_{n-k}(\mathcal{C})) &= \lim_{\epsilon \rightarrow \infty} \frac{1}{\epsilon^n} \mathbb{E} \left(\int_{\{\boldsymbol{\tau} \in [0,1]^k: |\mathbf{X}(\boldsymbol{\tau}) - \mathbf{u}_0|_m < \epsilon/2\}} \det \dot{\mathbf{X}}(\boldsymbol{\tau}) d\boldsymbol{\tau} \right) \\ &= \lim_{\epsilon \rightarrow \infty} \frac{1}{\epsilon^n} \int_{\{\mathbf{x} \in [0,1]^n: |\mathbf{x} - \mathbf{u}_0|_m < \epsilon/2\}} \int_{[0,1]^k} \mathbb{E} \left(\det \dot{\mathbf{X}}(\boldsymbol{\tau}) \mid \mathbf{X}(\boldsymbol{\tau}) = \mathbf{x} \right) f_{\mathbf{X}(\boldsymbol{\tau})}(\mathbf{x}) d\boldsymbol{\tau} d\mathbf{x} \\ &= \int_{[0,1]^k} \mathbb{E} \left(\det \dot{\mathbf{X}}(\boldsymbol{\tau}) \mid \mathbf{X}(\boldsymbol{\tau}) = \mathbf{u}_0 \right) f_{\mathbf{X}(\boldsymbol{\tau})}(\mathbf{u}_0) d\boldsymbol{\tau}. \end{aligned}$$

For a stationary case we get simply

$$(25) \quad \mathbb{E}(\mathcal{V}_{n-k}(\mathcal{C})) = \mathbb{E} \left(\det \dot{\mathbf{X}}(\mathbf{0}) \mid \mathbf{X}(\mathbf{0}) = \mathbf{u}_0 \right) f_{\mathbf{X}(\mathbf{0})}(\mathbf{u}_0).$$

The above argument can be generalized to obtain (4) and some further generalizations. Computing the mean number of empty envelope excursions is an example where such generalizations find applications. Using the notation of Section 3, let us define $\mathbf{X}(\boldsymbol{\tau}) = (E(\tau_1), E(\tau_2))$, for $\boldsymbol{\tau} = (\tau_1, \tau_2)$. The process and its envelope is jointly described by $\mathbf{V}(\cdot) = (E(\cdot), \theta(\cdot))$. The intensity of the empty envelope excursions described in the language of a generalized Rice formula is then given by

$$\nu_0^+(u) = \int_0^\infty \mathbb{E} \left(\{\mathbf{V}(\cdot) \in A\} \det \dot{\mathbf{X}}(0, \tau) \mid \mathbf{X}(0, \tau) = \mathbf{u} \right) f_{\mathbf{X}(0, \tau)}(\mathbf{u}), d\tau$$

where $\mathbf{u} = (u, u)$ and the property A means that there is an empty envelope excursion started at zero and concluded at τ , i.e. $\{\mathbf{V}(\cdot) \in A\} = \{E(s) > u, E(s) \cos \theta(s) < u, s \in (0, \tau)\}$. We also note that $\det \dot{\mathbf{X}}(0, \tau) = |\dot{E}(0) \cdot \dot{E}(\tau)|$. It is still an open mathematical problem to provide with the theoretical results that would formalize the argument sketched above

so it would apply to the above results. However, this example illustrates that the approach through such generalization of the classical Rice formula can lead to quite general tools for computing sampling distribution problems for fairly complex stochastic models. It should be mentioned that the above complex integral can be approximated numerically either by general Monte Carlo methods, or assisted by some analytical tools as in Ditlevson's work where the Slepian models was used.

In another application of the generalized Rice's formula, we have studied the statistical distributions for the envelope field. The intensities of the contour crossings are now defined as the lengths of the contour lines relatively to the rectangular area in which they are contained. It follows from generalized Rice's formula that the average ratio of this length to the area is given by

$$\mu^u = \mathbf{E} \left(\sqrt{E_x^2 + E_y^2} | E(\mathbf{0}) = u \right) \frac{u}{\lambda_{000}} e^{-u^2/(2\lambda_{000})}, \quad u > 0.$$

For consistency of the terminology we will still refer to this ratio as the intensity of the crossings. After some calculations involving the covariances between W , \hat{W} , W_x , W_y , \hat{W}_x , and \hat{W}_y [see also Baxevani et al. (2003) for mathematical details], one can obtain that this intensity is given by

$$\mu^u = \mathbf{E} \left(\sqrt{X_1^2 + X_2^2} \right) \frac{u}{\lambda_{000}} e^{-u^2/(2\lambda_{000})}, \quad u > 0,$$

where (X_1, X_2) is a Gaussian vector with variances $\lambda_{200} - \lambda_{100}^2/\lambda_{000}$, $\lambda_{020} - \lambda_{010}^2/\lambda_{000}$, respectively, and the covariance equal to $\lambda_{110} - \lambda_{100}\lambda_{010}/\lambda_{000}$. This functional form is identical to the intensity of crossing along a line although constants are different. In the special case of the sea surface we obtain some simplifications. First, it is usually assumed that the coordinates system for $W(\boldsymbol{\tau})$ is taken in such a way that $\lambda_{110} = 0$. Moreover, for spectra $S(\omega, \theta)$ exhibiting symmetry with respect to θ (which is the case for the spectra shown in Figure 1) we have also $\lambda_{010} = 0$. Consequently, X_1 and X_2 are independent Gaussian with variances $\lambda_{200} - \lambda_{100}^2/\lambda_{000}$ and λ_{020} , respectively and the formula for $\mathbf{E} \left(\sqrt{X_1^2 + X_2^2} \right)$ can be written more explicitly in terms of Legendre elliptical integral $\mathcal{E}(k) = \int_0^{\pi/2} \sqrt{1 - k^2 \sin^2 x} dx$ as follows

$$(26) \quad \mathbf{E} \left(\sqrt{X_1^2 + X_2^2} \right) = \sqrt{\frac{2}{\pi}} \cdot \frac{a_1^4}{a_2^3 \mathcal{E} \left(\sqrt{1 - a_1^2/a_2^2} \right)},$$

where $a_1 = \min(\lambda_{200} - \lambda_{100}^2/\lambda_{000}, \lambda_{020})$ and $a_2 = \max(\lambda_{200} - \lambda_{100}^2/\lambda_{000}, \lambda_{020})$.

We conclude with some derivation for the distribution of the velocity V for the envelope field when sampled on the contours. This distribution is explicitly given by the specifying the density of random variable Y in (18) as

$$(27) \quad f_Y(y) = \frac{\sqrt{C_1}}{4\pi C_2} \cdot y^2 \cdot e^{-\frac{y^2}{2}(1-C_1)} \left(K_0 \left(\frac{y^2}{2} C_1 \right) + K_1 \left(\frac{y^2}{2} C_1 \right) \right)$$

where K_0 and K_1 are modified Bessel functions of the second kind and the constants are defined as

$$C_1 = \frac{\lambda_{200} - \lambda_{100}^2}{\lambda_{020} \lambda_{000}},$$

$$C_2 = \mathbb{E} \sqrt{Z_x^2 + \frac{Z_y^2}{C_1}}.$$

Thus the constant C_2 can be written explicitly using (26). The above formula for the density follows easily from the following form of the sampling distribution that is a consequence of $\lambda_{010} = \lambda_{110} = \lambda_{011} = 0$ and can be obtained by using similar arguments as in Baxevani et al. (2003):

$$\mathbb{P} \left(V(x, y, 0) \leq v \mid (x, y) \in C_u^1 \right) = \frac{\mathbb{E} \left(\left\{ -\frac{1}{a} \left(b + \sqrt{a \cdot c - b^2} \cdot \frac{Z_t}{Z_x} \right) \leq v \right\} \sqrt{Z_x^2 + \frac{Z_y^2}{C_1}} \right)}{\mathbb{E} \sqrt{Z_x^2 + \frac{Z_y^2}{C_1}}},$$

where Z_x , Z_y , and Z_t are independent standard normal random variables.

REFERENCES

- [1] Adler, R.J. (1978) On the envelope of a Gaussian random field, *J. Appl. Prob.* **15**, pp. 502-513.
- [2] Adler, R.J. (1981) *The geometry of random fields*, Wiley, New York.
- [3] Baxevani, A., Podgórski, K., Rychlik, I. (2003) Velocities for moving random surfaces, *Prob. Eng. Mechanics*, **18**, pp. 251-271.
- [4] Bendat, J. S. (1964) Probability Functions for Random Responses: Prediction of Peaks, Fatigue Damage and Catastrophic Failures. *NASA technical report*.
- [5] Burcharth, H.F. (1980) A comparison of natural waves and model waves with special reference to wave grouping, *Proc. 17th Conf. on Coastal Eng., Sydney, Australia*, **3**, pp. 2992-3009.
- [6] Ditlevsen, O. (1994) Qualified envelope excursions out of an interval for stationary narrow-band gaussian process. *J. Sound and Vibration* **173**, pp. 309-327.
- [7] Ditlevsen, O., Lindgren, G. (1988) Empty envelope excursions in stationary gaussian processes. *J. Sound and Vibration* **122**, pp. 571-587.

- [8] Goda, Y. (1990) Random waves and spectra. *Handbook of Coastal and Ocean Engineering*, **1**, pp. 175-209.
- [9] Jiao G., Moan T. (1990) Probabilistic analysis of fatigue due to Gaussian load processes. *Prob. Eng. Mechanics*, **5**, pp. 76-83.
- [10] Lindgren, G. (1989) Slepian models for χ^2 -processes with dependent components with applications to envelope upcrossing. *J. Appl. Prob.*, **26**, pp. 36-49.
- [11] Longuet-Higgins, M. S. (1957) The statistical analysis of a random, moving surface. *Phil. Trans. Roy. Soc. A*, **249**, pp. 321-387.
- [12] Rayleigh, L. (1880) On resultant of a large number of vibrations of the same pitch and arbitrary phase. *Phil. Mag.*, **10**, pp. 73-78.
- [13] Rice, S. (1944) The mathematical analysis of random noise. *Bell Syst. Techn. J.*, **23**, pp. 282-332.
- [14] Rice, S. (1945) The mathematical analysis of random noise. *Bell Syst. Techn. J.*, **24**, pp. 46-156.
- [15] Rychlik, I. (1993) On the “narrow-band” approximation of expected fatigue damage. *Prob. Eng. Mechanics*, **8**, pp. 1-4.
- [16] Torsethaugen, K. (1996) Model for a doubly peaked wave spectrum Report No. STF22 A96204. *SINTEF Civil and Environm. Engineering*, Trondheim.
- [17] Vanmarcke, E. H. (1975) On the distribution of the first passage time for normal stationary random process. *J. Appl. Mechanics*, **42**, pp. 215-220.

DEPARTMENT OF MATHEMATICAL STATISTICS, LUND UNIVERSITY, BOX 118, 221 00 LUND, SWEDEN
E-mail address: `krys@maths.lth.se`

DEPARTMENT OF MATHEMATICAL STATISTICS, CHALMERS UNIVERSITY OF TECHNOLOGY, GÖTEBORG,
SWEDEN
E-mail address: `rychlik@chalmers.se`